

# INTERNATIONAL SOCIETY FOR SOIL MECHANICS AND GEOTECHNICAL ENGINEERING



*This paper was downloaded from the Online Library of the International Society for Soil Mechanics and Geotechnical Engineering (ISSMGE). The library is available here:*

<https://www.issmge.org/publications/online-library>

*This is an open-access database that archives thousands of papers published under the Auspices of the ISSMGE and maintained by the Innovation and Development Committee of ISSMGE.*

*The paper was published in the proceedings of the 10th International Conference on Physical Modelling in Geotechnics and was edited by Moonkyung Chung, Sung-Ryul Kim, Nam-Ryong Kim, Tae-Hyuk Kwon, Heon-Joon Park, Seong-Bae Jo and Jae-Hyun Kim. The conference was held in Daejeon, South Korea from September 19<sup>th</sup> to September 23<sup>rd</sup> 2022.*

# Laboratory verification of capillary barrier system using a small-scale model test

B.S. Kim & S.W. Park

*Department of Civil & Environ. Eng., Dankook Univ., Yongin, Korea*

S. Kato

*Graduate School of Engineering, Kobe University, Kobe, Japan*

**ABSTRACT:** A laboratory small-scale CB (SSCB) model test for a quick and efficient evaluation of the function of capillary barrier (CB) system in this study was proposed. In this model test, differently from previous studies, a side drainage flow in the direction of the inclined sand layer was set as the no-flow condition. The laboratory SSCB model tests were performed by considering three rainfall intensities (i.e., 20, 50, and 100 mm/h) under the lateral no-flow condition. The results showed that the larger the rainfall intensity, the shorter was the diversion length of the CB system. To evaluate the effectiveness of the SSCB model test proposed in this study, the diversion length was estimated by an empirical equation under the lateral flow condition based on hydraulic conductivity functions and soil water characteristic curves of sand and gravel, and then compared to the results of the SSCB model tests. It was hence demonstrated that the water-shielding performance of the CB system can be efficiently evaluated through SSCB model tests under the lateral no-flow condition, rather than through large-scale model tests.

**Keywords:** small-scale capillary barrier, lateral no-flow condition, diversion length, water-shielding, water retention characteristics.

## 1 INTRODUCTION

Capillary barrier (CB) systems, consisting of a layer of fine-grained material (e.g., silty or sandy soil) over one of coarse soil (e.g., gravel), provide a water-shielding effect, minimizing rainfall infiltration into the soil structure (Miyazaki, 1988). One of the advantages of the CB system is that it is eco-friendly because it generally consists exclusively of natural materials (e.g., silt, sand, and gravel). This system has been applied as a land-fill cover system for waste disposal sites or as an oxygen barrier to limit the production of acid mine drainage: it allows a safe discharge of rainwater infiltrated from the surface to the outside (Ross, 1990; Bussi re and Aubertin, 2003). Some researchers have also considered the application of the CB system for the maintenance of slope stability in soil structures since it can prevent rainwater infiltration into engineered slopes (Aubertin et al., 2009).

In the laboratory CB model tests, a large-scale model with a lateral length  $\geq 2.0$  m has been used: in this case, the water infiltration from the upper sand layer to the lower gravel layer occurred randomly. This large-scale model test requires a lot of time for its functioning; moreover, its fabrication is expensive, and the corresponding testing time is high, making it difficult to perform many CB model tests under different conditions. Thus, in this paper, we propose a laboratory small-scale CB (SSCB) model test that can quickly and efficiently

evaluate the water-shielding performance of a CB system. Differently from previous studies, here the SSCB system was characterized by setting the drainage condition in the flow direction of the inclined sand layer as the lateral no-flow (i.e., undrained) condition. This testing condition induced a quick infiltration of the water contained in the sand layer into the gravel layer in the flow direction, while the infiltrated water was drained from the gravel layer to the outside. Thus, the drainage condition of the SSCB model test reproduced an extreme condition for the CB system, which would result from the infiltration of rainfall from the surface layer. It is hence expected that the size of the CB model tests can be reduced and that their manufacturing time and corresponding testing time can be shortened.

To examine the effectiveness of the proposed SSCB model test under the lateral no-flow condition of the inclined sand layer, multiple tests were performed under three different rainfall intensities (i.e., 20, 50, and 100 mm/h). The diversion lengths that represent the water-shielding performance of the CB were estimated by the empirical equation of Steenhuis et al. (1991) under the lateral flow (i.e., drained) condition, based on the physical and water retention characteristics of the sand and gravel.

## 2 SOIL SAMPLES AND WATER RETENTION CHARACTERISTICS

### 2.1 Soil Sample

The soil samples used for the CB model tests were represented by Toyoura sand (standard sand in Japan) and silica sand No. 1 (as gravel material). The physical properties and hydraulic conductivities of the two soil samples are listed in Table 1. Notably, the saturated hydraulic conductivities ( $k_{sat}$ ) of Toyoura sand ( $\rho_d = 1.50$  g/cm<sup>3</sup>) and silica sand No. 1 ( $\rho_d = 1.64$  g/cm<sup>3</sup>) were obtained as  $1.45 \times 10^{-4}$  and  $2.44 \times 10^{-3}$  m/s, respectively.

Table 1. Physical properties and hydraulic conductivities of the soil samples.

Sample	Toyourea Sand	Silica Sand No.1
$\rho_s$ (g/cm <sup>3</sup> )	2.64	2.65
$D_{50}$ (cm)	1.69	4.65
$\rho_{d \max}$ (g/cm <sup>3</sup> )	1.64	1.67
$\rho_{d \min}$ (g/cm <sup>3</sup> )	1.37	1.45
$C_u$	1.63	2.24
$C_c$	0.97	0.84
$k_{sat}$ (m/s)	$1.45 \times 10^{-4}$	$2.44 \times 10^{-3}$

Note:  $\rho_s$ : Soil particle density,  $D_{50}$ : Mean particle size,  $\rho_{d \max}$ : Maximum dry density,  $\rho_{d \min}$ : Minimum dry density,  $C_u$ : Uniformity coefficient,  $C_c$ : Curvature coefficient,  $k_{sat}$ : Saturated hydraulic conductivity

### 2.2 Water Retention Characteristics

To obtain the SWCCs of Toyoura sand and silica sand No. 1, water retention tests through the continuous pressurization method were performed (Kim et al. 2021). Cylindrical specimens of 50 mm in diameter and 50 mm in height, with dry densities of 1.50 g/cm<sup>3</sup> and 1.64 g/cm<sup>3</sup>, were used for these tests. Figure 1(a) shows the fitted SWCCs resulting from the drying path of Toyoura sand and the wetting path of silica sand No. 1 (Fredlund and Xing, 1994a). An AEV of 2.30 kPa and an air expulsion value of 0.05 kPa were derived for Toyoura sand and silica sand No. 1, respectively. By comparing the SWCCs of the two soils, the different suction values indicate that the soils have distinct water retention capacities (of the water that infiltrates the sand layer). On the other hand, the relative hydraulic conductivities ( $k_r$ ) of the Toyoura sand and silica sand No. 1 under the unsaturated condition in this study were estimated based on the equation proposed by Fredlund et al. (1994b). Figure 1(b) shows the results of the hydraulic conductivities of Toyoura sand and silica No. 1. It was found that the hydraulic conductivity of Toyoura sand is larger for the suction value of about 0.07 kPa or more, which is the intersection of the two results. This difference can also be understood in relation to the CB

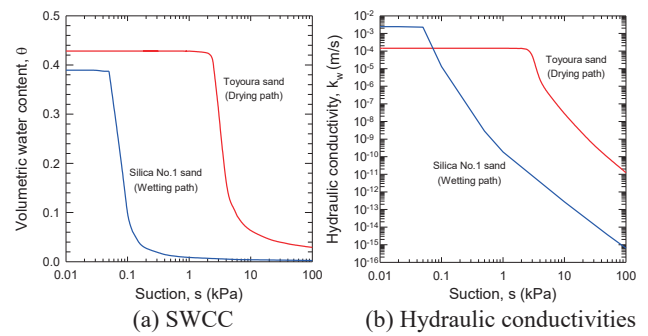


Fig. 1. SWCCs and Hydraulic conductivities of two soil samples used.

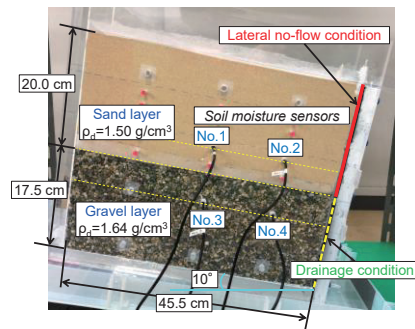


Fig. 2. Setting condition in the laboratory SSCB model test.

system's capability of retaining infiltrated water.

## 3 LABORATORY SSCB MODEL TEST UNDER THE LATERAL NO-FLOW CONDITION

### 3.1 Laboratory SSCB Model Test

The apparatus used for the CB model test included a water supply tank, a rainfall apparatus, and a soil tank. The inside of the soil tank was 45.5 cm long, 47.0 cm high, and 15.0 cm wide; moreover, the thickness of the acrylic material was 20 mm. The sand and gravel layers were 20.0 cm and 17.5 cm high, respectively as shown in Fig. 2; moreover, their initial dry densities ( $\rho_{di}$ ) were 1.50 g/cm<sup>3</sup> and 1.64 g/cm<sup>3</sup>, respectively. Differently from past studies conducted under the lateral flow condition, some material (i.e., tarpaulin) was installed to prevent drainage on the right side of the flow direction in the sand layer. To ensure the drainage of water that infiltrated from the sand layer to the gravel layer, the right side of the gravel layer was set as a drainage condition. Thus, the condition in the SSCB model test reproduces the extreme condition under which breakthrough forcibly occurs in the CB system. In other words, through the proposed SSCB model test, we expected to be able to quickly examine the performance of the CB system under certain test conditions.

Four soil moisture sensors (EC-5, Decagon Devices Co.), allowing the measurement of the volumetric water content 50 mm above and below the interface between the sand and gravel layers, were installed in the apparatus of the SSCB model test. The rainfall intensity

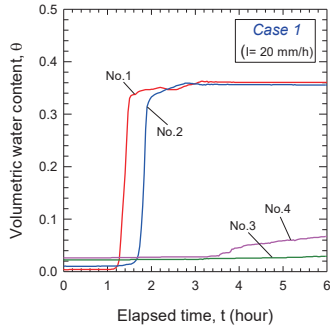


Fig. 3. Measured volumetric water contents ( $\theta$ ) for Case 1.

conditions were the following: 20 mm/h (Case 1), 50 mm/h (Case 2), and 100 mm/h (Case 3). The slope angle of the soil tank was  $10^\circ$ , and the performance of the CB system was evaluated for 6 h.

### 3.2 Infiltration behavior in the SSCB model test

Figure 3 shows the results of the volumetric water contents ( $\theta$ ) measured by the EC-5 sensors for Case 1 ( $I=20$  mm/h). It was observed that the measured values of sensors No. 3 and No. 4 after the breakthrough commonly increased up to 6 h. This tendency corresponds to a change according to the contact area with the sensor in the water infiltration paths. Thus, the infiltration path after 6 h in this study was also investigated, and the occurrence of an additional water infiltration path was not confirmed. At  $t=75$  min, sensor No. 1 showed the fastest response, indicating a rapid increase in the volumetric water content. Meanwhile, sensor No. 2 reported a rapid increase in the volumetric water content 10 min later than sensor No. 1; after which the volumetric water content appeared to quickly reach the saturated condition. These results indicate that the sand layer became saturated after 180 min. Sensor No. 3 did not show any response during the test. Finally, sensor No. 4 showed a gradual increase in the volumetric water content after 210 min, demonstrating the occurrence of a breakthrough at that time. On the other hand, in Cases 2 and 3, since the rainfall intensity was greater than that of Case 1, the response time (that is, time of breakthrough occurrence) of sensor Nos. 3 and 4 were 85 and 45 min, respectively.

### 3.3 Diversion Lengths in the SSCB Model Test

Figure 4 shows a sample situation in which a breakthrough occurred under the lateral no-flow condition. Here, the area comprised between [A] and [B] corresponds to the size of the model used for the laboratory model test. The breakthrough point was not easy to identify, because water infiltration from the interface between the sand and the gravel layers did not occur regularly over time. In addition, to determine the pattern of rainfall infiltration according to the sensor responses, we defined two types of diversion lengths in the SSCB model test as shown in Fig. 4(a). One of them

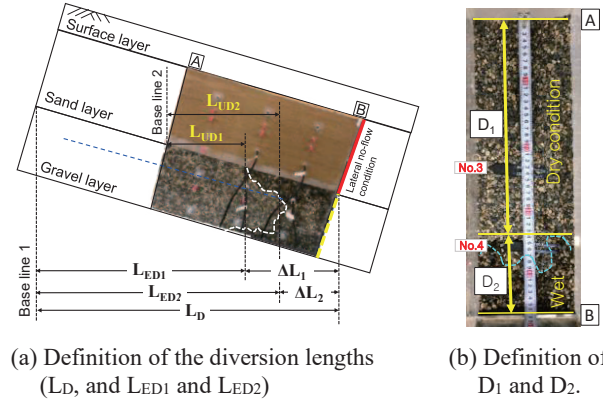


Fig. 4. Definition of each length in the SSCB model test under the lateral no-flow condition.

is the distance,  $L_{UD1}$  (i.e., the undrained diversion length), which was measured at the position of breakthrough occurrence from base-line 2 (at the interface between the sand and gravel layers). After the completion of the model test (at  $t=360$  min), the  $L_{UD1}$  values for each case were determined based on the infiltration of water from the front and back sides of the model under steady conditions. The  $L_{UD1}$  for Cases 1, 2, and 3 were 13.5 cm, 11.7 cm, and 0 cm, respectively. After the completion of the model test, the sand and gravel layers were carefully dismantled up to the location of sensors installed in the gravel layer; then, the lengths of  $D_1$  and  $D_2$  were measured as shown in Fig. 4(b). Here, the lengths of  $D_1$  and  $D_2$  correspond to the dry and wet areas, respectively. The  $D_1$  values for Cases 1, 2, and 3 were 25.2 cm, 11.3 cm, and 0 cm, respectively. The  $L_{UD2}$  values were calculated using the following formula:  $L_{UD2} = D_1 \cdot \cos\Phi$ , where  $\Phi$  is the slope angle, and those for Cases 1, 2, and 3 were 24.8 cm, 11.2 cm, and 0 cm, respectively.

### 3.4 Diversion Length on the SSCB Model Test

The existing diversion length ( $L_D$ ) under the lateral flow (drained) condition can be derived, like in past studies, by using Eq. (1) of Steenhuis et al. (1991).

$$L_D = \tan \Phi \cdot \left\{ \frac{1}{b} \left( \frac{1}{\kappa} - 1 \right) + \frac{1}{\kappa} (h_{ae} - h_{ex}) \right\} \quad (1)$$

where  $b$  was derived from the equation of unsaturated hydraulic conductivity and from the relationship of  $k = k_{sat} \cdot \exp(b\psi_m)$  (here,  $k_{sat}$ : the saturated hydraulic conductivity and  $\psi_m$ : the suction ( $h$ , cmH<sub>2</sub>O)). Moreover,  $\Phi$  is the slope of the interface,  $\kappa$  was derived from the relationship  $\kappa = q_v/k_{sat}$ , (here,  $q_v$ : the flux of water entering the soil),  $h_{ae}$  is the air entry value (AEV) of sand, and  $h_{ex}$  is the air expulsion value of gravel.

Table 2 summarizes the input parameters and results of the diversion length estimated by Eq. (1). Meanwhile, the lengths of  $\Delta L_1$  and  $\Delta L_2$  were used to identify the wet areas of the gravel layer that formed due to breakthrough (Fig. 4(a)). By considering  $\Delta L_1 = L_{st} - L_{UD1}$

Table 2. Input parameters and results of the diversion length estimation for Eq. (1).

$q_v$ (mm/h)	$k_{sat}$ (cm/s)	$\kappa$	$b$	$\Phi$ (°)	$h_{ae}$ (cm)	$h_{aex}$ (cm)	$L_D$ (cm)
20	$1.45 \times 10^{-2}$	0.038	0.13	10	24.5	0.5	145.5
50		0.096					56.8
100		0.192					27.7

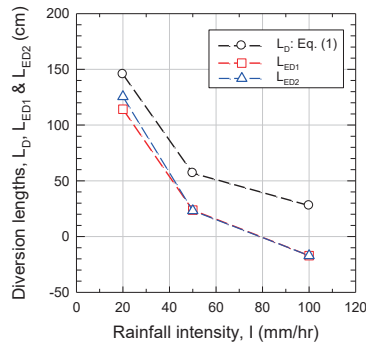


Fig. 5. Comparison of the measured and estimated diversion lengths.

and  $\Delta L_2 = L_{st} - L_{UD2}$ , the following values were derived for  $\Delta L_1$  and  $\Delta L_2$ : 31.3 and 20.0 cm (Case 1), 33.1 and 33.6 cm (Case 2), and 44.8 and 44.8 cm (Case 3), respectively. The horizontal length of the soil tank of  $L_{st}$  was defined by considering the slope angle (i.e.,  $L_{st} = 45.5 \times \cos \Phi$ , in cm). The effective diversion lengths ( $L_{ED1}$  and  $L_{ED2}$ ) became smaller under the lateral no-flow condition:  $L_{ED1} = L_D - \Delta L_1$  and  $L_{ED2} = L_D - \Delta L_2$  (Fig. 4(a)). Here,  $L_{ED1}$  represented the diversion length in the level of the interface between two soil layers, while  $L_{ED2}$  represented the diversion length in the sensor installation level in the gravel layer. We obtained the following values for  $L_{ED1}$  and  $L_{ED2}$ : 114.2 and 125.5 cm (Case 1), 23.7 and 23.1 cm (Case 2), and -17.1 and -17.1 cm (Case 3), respectively. Here, negative values of  $L_{ED1}$  and  $L_{ED2}$  (e.g., -17.1 and -17.1 cm for Case 3) indicated that the diversion length could not be formed under extreme rainfall ( $I = 100$  mm/h), which means there is no water-shielding performance of the CB system.

The resulting effective diversion lengths (i.e.,  $L_{ED1}$  and  $L_{ED2}$ ) in the CB system were 21.5% and 13.8% lower in Case 1 and 58.3% and 59.2% lower in Case 2, respectively, than the  $L_D$  values estimated by Eq. (1) as shown in Fig. 5. In Case 3, under  $I = 100$  mm/h, although the occurrence of a diversion length ( $L_D = 27.7$  cm) was predicted by the empirical formula, no diversion length could be observed during the SSCB model test. The obtained results indicate that the water-shielding performance of the CB system can be efficiently evaluated through the SSCB model test under the lateral no-flow condition, rather than through large-scale model tests. It was concluded that the application of the results of the SSCB model test in the slope design of soil structures based on the CB system would be helpful for

improving slope stability.

#### 4 CONCLUDING REMARKS

In this study, the laboratory SSCB model tests by setting the lateral no-flow condition of the inclined sand layer were performed to efficiently evaluate the water-shielding performance of the CB system. Since the SSCB model was smaller than the large-scale models, it was expected that its production work and testing would have a lower cost, and the testing time was relatively short. The diversion lengths in the SSCB model test of this study were measured based on two criteria (i.e.,  $L_{UD1}$  and  $L_{UD2}$ ). The  $L_{UD1}$  values obtained for Cases 1, 2, and 3 were 13.5 cm, 11.7 cm, and 0 cm, respectively; meanwhile, the  $L_{UD2}$  values were 24.8 cm, 11.2 cm, and 0 cm, respectively. The diversion lengths ( $L_D$ ) for each case estimated by Eq. (1) were 145.5 cm, 56.8 cm, and 27.7 cm, respectively. The effective diversion lengths (i.e.,  $L_{ED1}$  and  $L_{ED2}$ ) for the real CB system were derived were 114.2 and 125.5 cm, 23.7 and 23.1 cm, and -17.1 and -17.1 cm, respectively. Based on the obtained results, the water-shielding performance of the CB system can be efficiently evaluated by conducting the proposed SSCB model tests under the lateral no-flow condition, rather than through large-scale model tests. Furthermore, the application of the results of the SSCB model test to the slope design of soil structures based on the CB system would be helpful for improving slope stability.

#### ACKNOWLEDGEMENTS

This work was partly supported under the framework of an international cooperation program managed by the National Research Foundation of Korea (NRF-2021K2A9A1A01102233).

#### REFERENCES

- Aubertin, M., Cifuentes, E., Apithy, S.A., Bussi re, B., Molson, J., and Chapuis, R.P. 2009. Analyses of water diversion along inclined covers with capillary barrier effects. *Can. Geotech. J.* 46, 1146-1164.
- Bussi re, B., Aubertin, M., and Chapuis, R.P. 2003. The behavior of inclined covers used as oxygen barriers. *Can. Geotech. J.* 40, 512-535.
- Fredlund, D.G. & Xing, A. 1994a. Equations for the soil-water characteristic curve. *Can. Geotech. J.* 31, 521-532.
- Fredlund, D.G., Xing, A. and Huang, S. 1994b. Predicting the permeability function for unsaturated soils using the soil-water characteristic curve. *Can. Geotech. J.* 31, 533-546.
- Kim, B.S., Hatakeyama, M., Park, S.W., Park, H.S., Takeshita, Y., and Kato, S. 2021. Assessment of water retention test by continuous pressurization method, *Geotech. Test. J.* 44, 274-289.
- Ross, B. 1990. The diversion capacity of capillary barriers, *Water Resour. Res.* 26, 2625-2629.
- Steenhuis, T.S., Parlange, J.-Y., and Kung, K.-S. 1991. Comment on "The diversion capacity of capillary barriers" by Benjamin Ross. *Water Resour. Res.* 27, 2155-2156.